frontiers | Frontiers in Earth Science

ORIGINAL RESEARCH
published: 16 May 2022
doi: 10.3389/feart.2022.906782

Types and Eruption Patterns of the Carboniferous Volcanic Edifices in the Shixi Area, Junggar Basin

Abulimiti Yiming[1], *Baoli Bian*[1], *Longsong Liu*[1], *Hailong Chen*[1], *Xuanlong Shan*[2], *Ang Li*[2]* *and Jian Yi*[2]

[1]Research Institute of Exploration and Development, Xinjiang Oilfield Company, PetroChina, Karamay, China, [2]College of Earth Sciences, Jilin University, Changchun, China

The types of volcanic edifices and volcanic eruption patterns control the accumulation and distribution of oil and gas. By means of drillings, seismic data, and geochemical analysis, the types and distribution of the Carboniferous volcanic edifices in the Shixi area of Junggar Basin were studied, the formation mechanism of magma was clarified, and the eruption patterns of volcanoes were investigated. The results show that the types of the Carboniferous volcanic edifices in the Shixi area mainly include stratovolcanic edifices, shield basic volcanic edifices, and mound superimposed volcanic edifices. Stratovolcanic edifices and mound superimposed volcanic edifices are developed around the Shixi fault, while single stratovolcanic edifices are developed around the Mobei fault. Shield basic volcanic edifices are only developed in the south of the Shixi area. Vertically, volcanic edifices are mainly developed on the hanging walls of the faults. When the faults develop, the volcanic vents are dendritic, forming mound superimposed volcanic edifices in space. On the plane, there are more volcanic edifices in the Shixi salient than in the Mobei salient. Intermediate-acid volcanic edifices are distributed in beaded shapes along one side of the Shixi fault and the Mobei fault, while basic volcanic edifices are distributed in sheet shapes on both sides of the Dinan fault. In the early Carboniferous, the Shixi area was in the island arc environment under the subduction of the oceanic crust. The basic magma came from the melting of the subduction plate, and the intermediate-acid magma came from the partial melting of the crust. In the late Carboniferous, the extensional environment formed by the retraction of the subduction plate led to the formation of large-scale volcanic eruptions. The extensional environment formed by the retreat of the subduction plate in the later stage resulted in large-scale volcanic eruptions.

Keywords: Junggar Basin, Shixi area, Carboniferous, volcanic edifices, eruption patterns, magma source

OPEN ACCESS

Edited by:
Hu Li,
Southwest Petroleum University, China

Reviewed by:
Jianhua He,
Chengdu University of Technology, China
Saipeng Huang,
University of Barcelona, Spain

***Correspondence:**
Ang Li
liang2020@jlu.edu.cn

Specialty section:
This article was submitted to Structural Geology and Tectonics, a section of the journal Frontiers in Earth Science

Received: *29 March 2022*
Accepted: *13 April 2022*
Published: *16 May 2022*

Citation:
Yiming A, Bian B, Liu L, Chen H, Shan X, Li A and Yi J (2022) Types and Eruption Patterns of the Carboniferous Volcanic Edifices in the Shixi Area, Junggar Basin. Front. Earth Sci. 10:906782. doi: 10.3389/feart.2022.906782

1 INTRODUCTION

Volcanic oil and gas, as an important unconventional source of oil and gas, has effectively alleviated the energy shortage in China and become a realistic replacement field for oil and gas exploration (Chen et al., 2015; Ma et al., 2019). Since the 1980s, China's onshore volcanic oil and gas exploration has entered a stage of rapid development, and the proved geological reserves have been greatly improved. Industrial oil and gas flows have been found in the Carboniferous-Permian volcanic rocks in Songliao Basin, Bohai Bay Basin, Junggar Basin, and Santanghu Basin (Zou et al., 2008; He et al.,

2009; Meng et al., 2021). In 2008, the Xinjiang oilfield discovered the Kelamili gas field with resources of 100 billion cubic meters in the Carboniferous volcanoes in the central Junggar Basin, which opened a new prospect of volcanic oil and gas exploration and development in the Junggar Basin. Previous studies have focused on the tectonic setting, chronological characteristics, and hydrocarbon accumulation mechanism of volcanic rocks in the Junggar Basin, which has played an important supporting role in promoting the exploration and development of volcanic oil and gas reservoirs in the Junggar Basin (Zhang et al., 2015; Huang et al., 2020; You et al., 2021).

The Shixi area is located in the Luliang uplift, and the proven petroleum reserves of the Carboniferous system are 38.94 million tons. The high-quality volcanic reservoirs are mainly volcanic breccia, volcanic agglomerate, and blowhole lava. The volcanic edifice controls the scale and distribution of volcanic lithologies and lithofacies, so it is very important to find out the eruption patterns and distribution laws of volcanic edifices for the exploration and development of volcanic oil and gas. Based on magma properties, lithological associations, volcanic edifice structures, and eruption patterns, previous studies have divided a variety of classification schemes of volcanic edifices. Tang et al. (2012) divided the volcanic edifices of the Yingcheng formation in the southern Songliao basin into rhyolitic lava volcanic edifices, rhyolitic clastic volcanic edifices, composite volcanic edifices, dacite lava volcanic edifices, and andesitic clastic volcanic edifices according to the magma properties and lithology. The Carboniferous volcanic edifices in the Ludong-Wucaiwan area of the Junggar Basin are divided into shield volcanic edifices, stratovolcanic edifices, calderas, lava domes, and cinder cones according to the structure and shape of volcanic edifices (Zhao and Shi, 2012). Huang et al. (2007) further divided conical volcanic edifices into single conical volcanic edifices, multi-conical volcanic edifices, and stacked conical volcanic edifices. At present, the research on volcanic eruption patterns mainly analyzes the relationships between volcanic eruptions and faults. Volcanic eruptions mainly include central eruptions, fissure eruptions, and fissure-central eruptions. The Permian magma erupted in the fissure type along the NE-trending faults in the southern Jianyang area of the Sichuan Basin (Xia et al., 2020). Qu (2019) divided the volcanic eruption patterns of the Yingcheng formation in the Xushen gasfield of the Songliao basin into central eruptions and fissure-central eruptions distributed along faults.

The Carboniferous volcanic rocks in the Shixi area are deeply buried and have undergone multiple stages of tectonic movements and weathering, resulting in hard-to-identify volcanic edifices due to serious deformation. By means of field geological survey, observation and description of drilling cores, and geophysical techniques, researchers have a deep understanding of the lithologies, lithofacies, and identification methods of volcanic edifices in this area (Yin et al., 2019; Dai et al., 2020; Lan et al., 2021; Li H. et al., 2021; Li, 2022). However, the research studies on volcanic edifice types and volcanic eruption patterns are a little insufficient. On the basis of summarizing previous achievements, drillings, seismic data, and geochemical analysis are used in this article to investigate the types and distribution of the Carboniferous volcanic edifices, the formation mechanism of magma, and the eruption patterns of volcanoes in the Shixi area. The results provide a geological basis for increasing oil and gas reserves and production in this area.

2 GEOLOGICAL BACKGROUND

The Shixi area is located in the Shixi salient and Mobei salient in the south of the Luliang uplift in the central Junggar Basin and adjacent to the west sag of the Pen 1 well and Shinan sag, respectively, in the north and south, which has superior oil and gas geological conditions (**Figure 1**). NE-trending and NW-trending faults are developed in this area, of which two NE-trending large basement faults (Shixi fault and Mobei fault) control the development of nose-shaped salients (Ma et al., 2013). In the early Carboniferous, the Luliang island arc was affected by oceanic crust subduction, resulting in large-scale volcanic eruptions and the development of a huge thickness of volcanic rock strata with a buried depth of more than 4,000 m (Wang L. et al., 2020). There are three eruption cycles in the upper Carboniferous in the Shixi area, of which the third cycle includes four stages of volcanic activities. Most wells are drilled in the third cycle, and the lithofacies are mainly characterized by overflow facies and explosive facies, which appear alternately and are dominated by overflow facies. The rock types of overflow facies mainly include basalt, andesite, dacite, and rhyolite. The explosive facies mainly develop volcanic breccia and tuff (**Figure 2**). The upper Carboniferous volcanic reservoirs are connected with hydrocarbon generation sags through basement faults, forming large-scale oil and gas reservoirs.

3 VOLCANIC EDIFICE TYPES

The upper Carboniferous volcanic rocks in the Shixi area are mainly intermediate-acid rocks, and a small number of basic rocks are developed in the south. Based on the lithology, structure, and shape, the volcanic edifices in the study area can be divided into various types. Intermediate-acid lavas are mostly interbedded with pyroclastic rocks to form mound-like stratovolcanic edifices. When volcanic vents are well developed in a certain region, mound superimposed volcanic edifices can be formed. In addition, the basic lava develops into large shield volcanic edifices.

3.1 Stratovolcanic Edifice

A stratovolcanic edifice, an interbedded volcanic structure composed of eruptive pyroclasts and overflow lavas, is formed by periodic central eruptions (Gao et al., 2019; Gong et al., 2019). The lavas of the stratovolcanic edifice in the Shixi area are mainly intermediate-acid lavas such as andesite, dacite, and rhyolite, which play the role of the framework of volcanic edifices (**Figure 3A**). The upper subfacies of lava develop blowhole belts, which can be regarded as favorable reservoirs for oil and gas (**Figure 4**). The eruptive pyroclasts are mainly volcanic

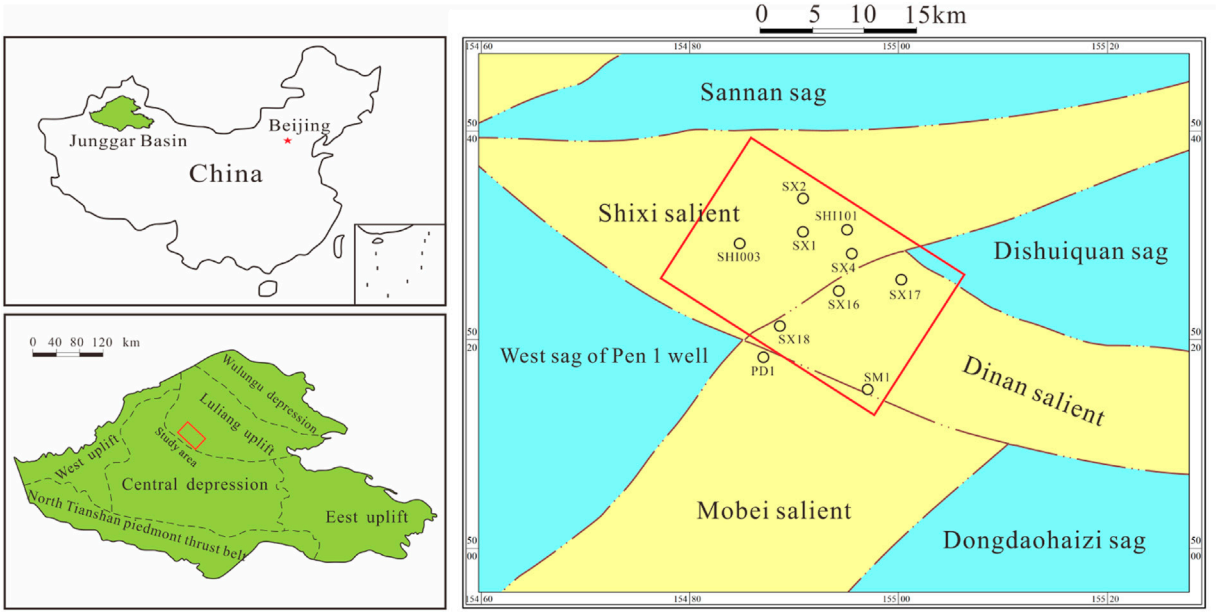

FIGURE 1 | Tectonic unit of the Junggar Basin and studying area.

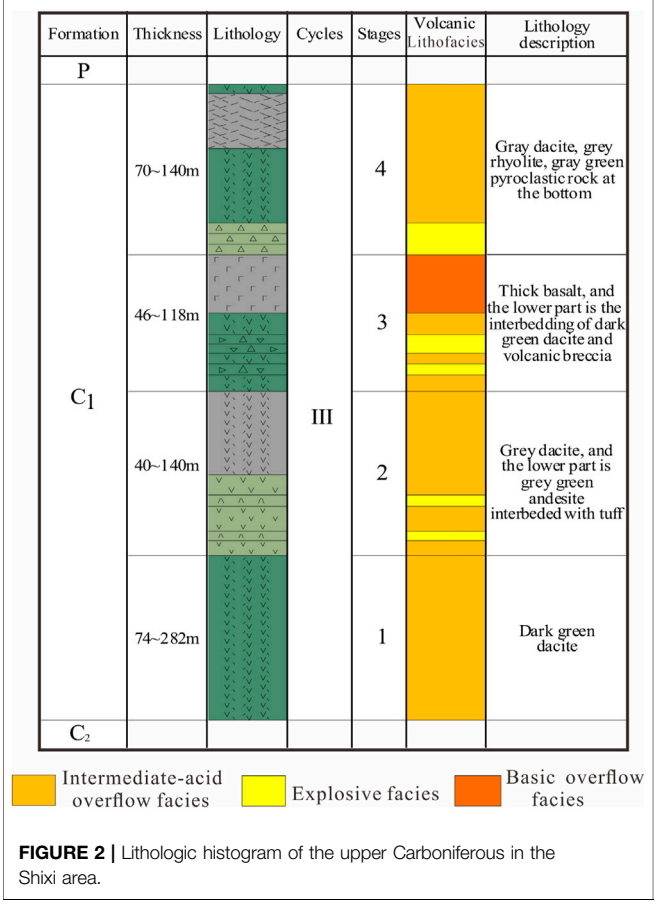

FIGURE 2 | Lithologic histogram of the upper Carboniferous in the Shixi area.

breccia, volcanic agglomerate, and a small amount of tuff. The thickness of lavas and pyroclasts is controlled by the intensity of eruption. Due to the high viscosity of intermediate-acid magma, stratovolcanic edifices usually have a large aspect ratio, showing the shapes of cones or mounds.

The stratovolcanic edifice is the most developed type of volcanic edifice in the Shixi area. In the seismic profile, it shows a mound-shaped seismic reflection shape and strong amplitude chaotic reflection and continuous reflection interbedding in the interior due to the lithology difference. The volcanic vent is located in the middle of the volcanic edifice. The interior of the volcanic vent shows disordered or blank seismic reflection, and the strata on both sides of the volcanic vent are inclined to both sides. Wells SX16 and SX18 in the study area were drilled into the proximal facies of volcanic edifices. The interbedded volcanic breccia with volcanic lava (andesite and dacite) can be seen in the SX16 well, which is a typical stratovolcanic edifice. The upper part of the SX18 well is volcanic breccia, and the lower part is dacite. Due to the influence of formation thickness and drilling depth, the interbedded structure of volcanic breccia and volcanic lava is not shown in the SX18 well.

3.2 Shield Basic Volcanic Edifice

Basic magma is characterized by low viscosity and high fluidity and forms shield volcanic edifices with a small aspect ratio and wide distribution (Hu et al., 2018). Basic magma often presents fissure eruptions along large faults, so basic volcanic edifices are distributed in a belt around the faults. When the magma flow is large or close to the volcanic vent, the shear stress is generated by

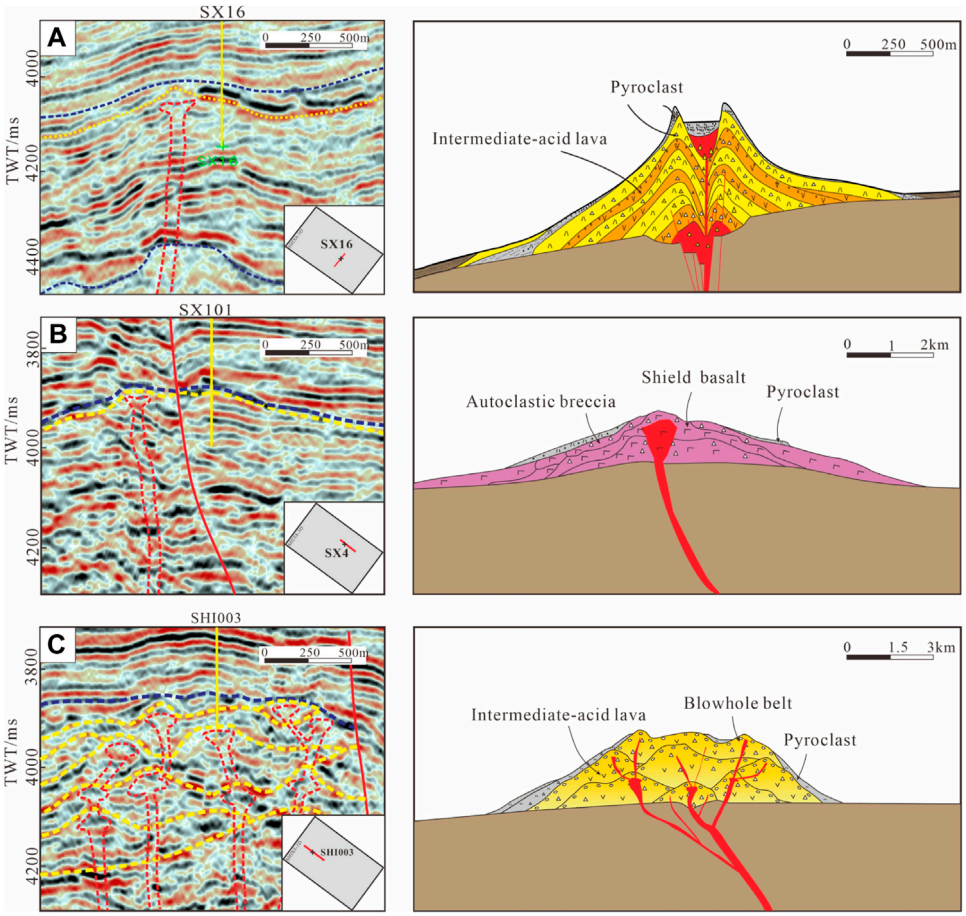

FIGURE 3 | Types and development models of Carboniferous volcanic edifices in the Shixi area.

the velocity difference between the top and bottom due to the fast condensation rate and slow flow speed at the top and the slow condensation rate and fast flow speed at the bottom, which leads to the formation of autoclastic breccia belts at the top of the magma (Luo et al., 2013; Li H. et al., 2020; Tang et al., 2020).

There are few shield basic volcanic edifices in the study area. It is only found that the Dinan fault in the south of the study area is a basic magmatic vent, and basalt is distributed in sheet shapes on both sides of the fault (**Figure 3B**). In the seismic profile, basalt shows a large thickness near the Dinan fault and gradually thinning far away from the fault, and the whole volcanic edifice is a shield. The seismic reflection axis has a strong amplitude, a moderate frequency, and good continuity. Thick basalt was drilled in wells SX101, SX4, and SX17 in the south of the study area. Multiple sets of basaltic autoclastic breccia belts were developed in the SX101 well close to the volcanic vent. However, wells SX4 and SX17 are far away from the volcanic vents, so there are no autoclastic breccia belts, and the lithology of these two wells is thick basalt with blowholes at the top (**Figure 4**).

3.3 Mound Superimposed Volcanic Edifice

When volcanic vents are well developed in a certain region, a composite volcanic edifice with multiple volcanic mounds superimposed on each other can be formed. Volcanic vents are inherited and extend in tree shapes in space. Cryptoexplosive breccia belts are often developed in mound superimposed volcanic edifices (Yi et al., 2011; Wang X. Y. et al., 2020). The mound superposed volcanic edifice in the study area is dominated by intermediate-acid overflow facies, intercalated with explosive facies (**Figure 3C**). The scale of a single volcanic mound is small, but the thickness of a composite volcanic edifice is large. Because the upper subfacies of the overflow facies often developed blowhole belts, there were several sets of blowhole lavas in the vertical direction of this volcanic edifice, which is regarded as a high-quality volcanic reservoir and conducive to the enrichment of oil and gas. In the study area, the mound superposed volcanic edifices mainly occur in the area where faults are developed, and the large basement faults and secondary faults provide channels for the upwelling magma. In the seismic profile, the volcanic mounds are obviously superposed vertically, which has the characteristics of multi-stage volcanic eruptions. Seismic reflection is disordered because of the development of faults and volcanic vents. The interface between the lava and pyroclast is characterized by discontinuous strong reflection. Well SHI003 was drilled into the shallow layer

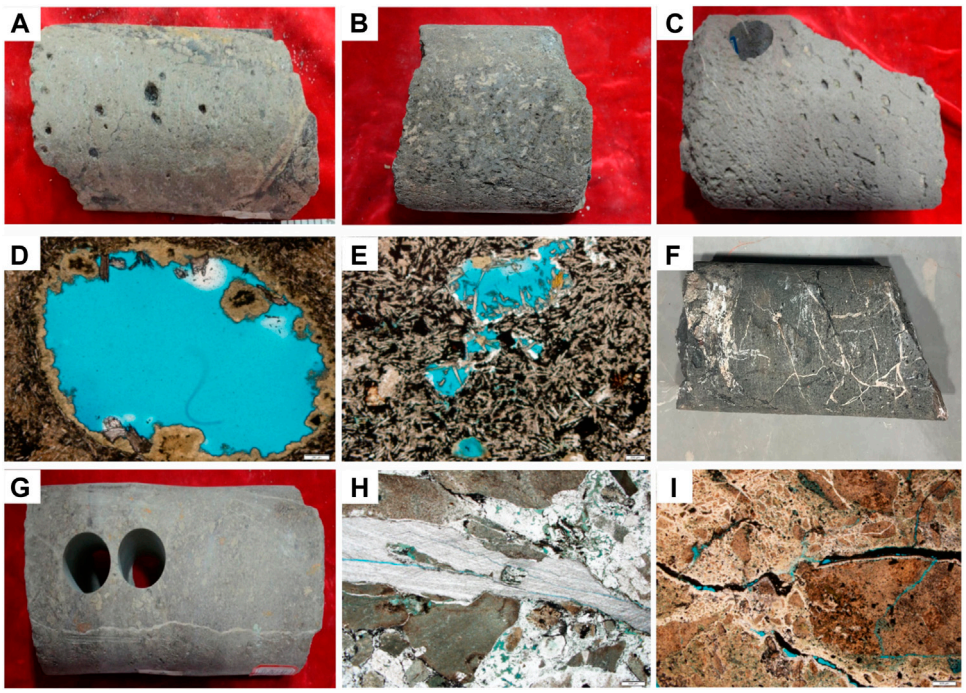

FIGURE 4 | Blowholes in upper subfacies of the lava and fractures in volcanic rocks. **(A, B)** Blowholes in andesite, SX16, 4805.5 m and SX4, 4822.4 m; **(C)** blowholes in basalt, SX4, 4720.2 m; **(D)** microscopic characteristics of blowholes in andesite, SX16, 4805.5 m; **(E)** microscopic characteristics of blowholes in basalt, SX4, 4720.8 m; **(F, G)** volcanic rock fractures, SX18, 5179.6 m and SX3, 4720.8 m; **(H, I)** microscopic characteristics of volcanic rock fractures, SX3, 4721.06 m and SX3, 3867.5 m.

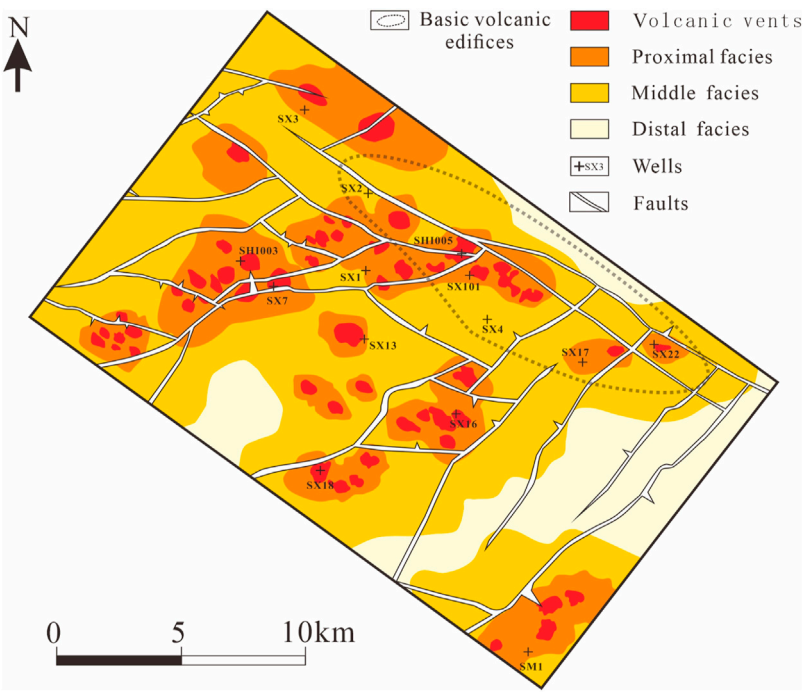

FIGURE 5 | Distribution of upper Carboniferous volcanic edifices in the study area.

of mound superimposed volcanic edifices, and the lithology was a set of thick andesite because this well was far away from the volcanic vents.

4 VOLCANIC EDIFICES AND FAULTS

As the channels for magma, faults control the eruption of volcanoes. The Shixi fault, the Mobei fault, and the Dinan fault are three large basement faults which control the development of nose-shaped salients in the Shixi area and are also channels of magma eruption. Through the interpretation of seismic data, the volcanic edifice distribution of the upper Carboniferous in the Shixi area is shown in **Figure 5**. Faults not only control the types of volcanic edifices but also affect the distribution of volcanic edifices.

4.1 Relationships Between Volcanic Edifice Types and Faults

Volcanic eruptions mainly include central eruptions and fissure eruptions. The intermediate-acid magma with high viscosity upwelled along the Shixi fault and Mobei fault in the way of "squeezing toothpaste" to form the central eruption and accumulated with the pyroclast to form the volcanic mounds. Therefore, the volcanic edifices developed around the Shixi fault and the Mobei fault are stratovolcanic edifices and mound superimposed volcanic edifices. In addition, the development degree of fault controls the types of volcanic edifices in the study area. The structure conditions of the Shixi salient in the west of the Shixi area are relatively complicated. The development degree of NW-trending faults in the Shixi salient is significantly higher than that of the Mobei salient, and the NW-trending faults are intersected with the Shixi faults, resulting in the development of secondary faults near the basement faults, which are conducive to the formation of volcanic vents (Li, 2019). Therefore, the mound superimposed volcanic edifices are well developed in the Shixi salient, while there is no such volcanic edifice in the Mobei salient and there are mostly single stratovolcanic edifices. In addition, the scale of a mound superimposed volcanic edifice formed by multi-stage eruptions is larger than that of a single stratovolcanic edifice. Fractures in volcanic rocks are well developed in the areas where faults are well developed and complex (**Figure 4**). The viscosity of basic magma is less than that of intermediate-acid magma, which makes it easier to form fissure eruptions along the fault. The Dinan fault is a banded volcanic vent with basic magma overflow, and the shield basic volcanic edifice is distributed in the NW direction along the Dinan fault. The distribution of basic volcanic edifices on the plane is significantly larger than that of stratovolcanic edifices and mound superimposed volcanic edifices.

4.2 Relationships Between Volcanic Edifice Distribution and Faults

Deep magma usually erupts, overflows, or emplaces along weak zones of the strata, and these weak zones are the basement faults and associated faults with long-term succession activities (Shan et al., 2011; Lu et al., 2019; Fan et al., 2020; Lan et al., 2021; Meng et al., 2021). The Shixi fault, Mobei fault, and Dinan fault, as three large basement faults in the Shixi area, are the main magma channels and control the distribution of volcanic edifices. Vertically, the volcanic edifice is mainly developed on the hanging walls of the faults (Shixi salient and Mobei salient), which results in the thickness of volcanic rocks on the salients being obviously larger than that on the sags. After rising along the main channel, the intermediate-acid magma erupted from the surface by the secondary faults or strata melt-through. When the secondary faults are well developed near the basement fault, dendritic volcanic vents are easily formed, and multiple volcanic edifices are superimposed in space. Conversely, when secondary faults are not developed, a single or small number of volcanic edifices are formed (**Figure 6**). In the plane, intermediate-acid volcanic edifices are distributed in beads along one side of the Shixi fault and Mobei fault (**Figure 7**). The number of volcanic edifices in the Shixi salient is more than that in the Mobei salient. The proximal facies and middle facies of volcanic edifices are mainly developed in the Shixi salient, while there are proximal facies, middle facies, and distal facies of volcanic edifices in the Mobei salient. Some small faults such as the east fault of well SX17 and the west fault of the SM1 well do not cut deep into the basement and are far away from the Mobei fault, so these faults cannot become volcanic vents. It can also be seen from the distribution map of volcanic edifices that the volcanic edifices around small faults are not developed. In general, the development of volcanic edifices in the west of the Shixi area is significantly stronger than that in the east, and the volcanic edifices between the two salients are not developed. The basic volcanic edifices are distributed in sheet shapes on both sides of the Dinan fault. There are few intermediate-acid volcanic edifices near the Dinan fault, and only a few volcanic vents are developed at the intersection with the Shixi fault. Therefore, according to the relationship between volcanic edifices and faults, the Shixi area can be divided into three volcanic belts: the Shixi fault intermediate-acid volcanic belt, Mobei fault intermediate-acid volcanic belt, and Dinan fault basic volcanic belt.

5 VOLCANIC ERUPTION

5.1 Magma Formation Mechanism

In order to study the formation and evolution of magma in the Shixi area, the volcanic rocks were systematically sampled, and the major and trace element analysis and Sr-Nb isotope tests were carried out. In the Total Alkali and Silica (TAS) diagram and Nb/Y-Zr/TiO_2 diagram, most samples are in the andesite and dacite area, two samples are in the rhyolite area, and one sample is in the basalt area (**Figure 8**). In this study, whole-rock geochemical data (**Figure 9**) and Sr-Nd isotopic data (**Figure 10**) were used to discuss the magma formation mechanism of the three types of volcanic rocks with different geochemical properties.

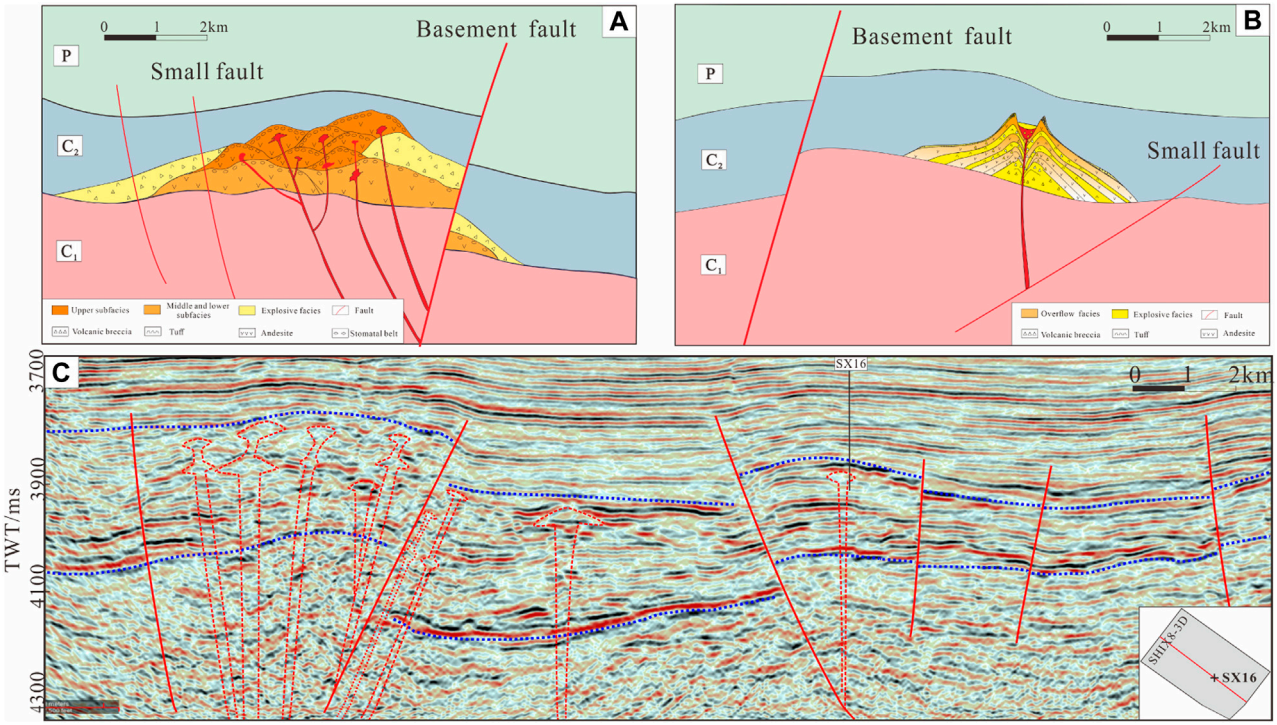

FIGURE 6 | Relationship between faults and volcanic edifices in the Shixi area. **(A)** When faults develop, mound superimposed volcanic edifices are developed; **(B)** when faults are not developed, single stratovolcanic edifices are developed; **(C)** seismic profile through well SX16.

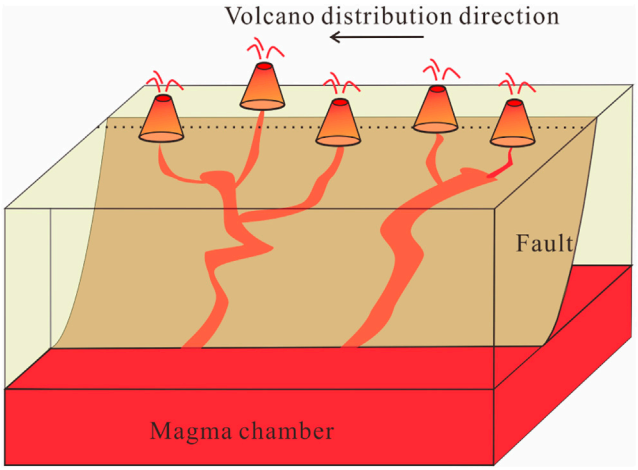

FIGURE 7 | Beaded distribution of intermediate-acid volcanic edifices along faults.

5.1.1 Formation Mechanism of Basic Magma

The Mg# (0.443) of basalt samples is relatively low, which reflects that the basalt underwent a very weak degree of fractional crystallization. At the same time, these samples have the characteristics of a low Th/Ce value (0.038) and a low Th/La value (0.080), indicating that the assimilation and contamination of the continental crust during the evolution of basic magma are very little. The low $(^{87}Sr/^{86}Sr)_i$ value (0.70448) and the high εNd(t) value (6.31) of the basic samples also prove that the evolution of the basalt has nothing to do with the contamination of the crust. The isotopic composition indicates that the magma originated from the depleted mantle. There are no obvious negative anomalies of Nb and Ta, and the trace element composition model is similar to that of oceanic island basalt (OIB). Combined with the characteristics of $(Th/Nb)_N$ less than 1 and the depleted Sr-Nd isotope, it is speculated that the basic magma originated from the asthenosphere mantle (Aldanmaz et al., 2000; Tamura et al., 2014; Li et al., 2019; Zhu et al., 2019; Li S. B. et al., 2021).

5.1.2 Formation Mechanism of Intermediate Magma

Andesite and dacite samples are characterized by low MgO contents (0.314–3.14), indicating that they are not caused by partial melting of subduction plate materials from the enriched mantle. There are relatively few basic volcanic rocks in the upper Carboniferous in the Shixi area, and their petrographic characteristics do not contain ferromagnetic inclusions, so it is ruled out that the intermediate magma came from the mixing of basic magma and acid magma. The La/Sm values of the samples increase gradually with the increase of La contents, reflecting that the magma was derived from partial melting rather than fractional crystallization (Geng et al., 2011; Safonova et al., 2015; Li L. et al., 2020). The samples are enriched in large ion

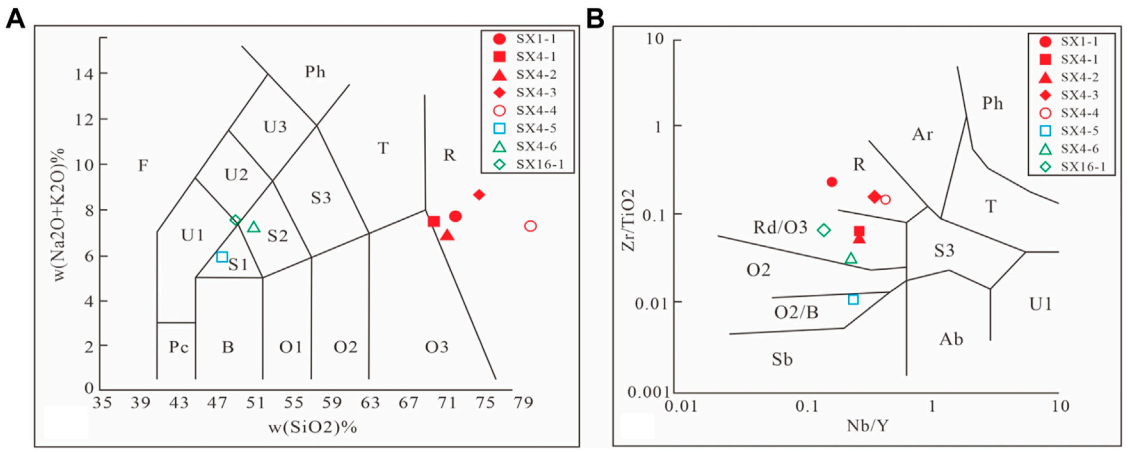

FIGURE 8 | TAS diagram **(A)** and Nb/Y-Zr/TiO_2 lithology classification diagram **(B)** of Carboniferous volcanic rocks in the Shixi area (Pc-Picrite; B-Basalt; O1-Basaltic Andesite; O2-Andesite; O3-Dacite; R-Rhyolite; S1-Trachybasalt; S2-Basaltic Trachyandesite; S3-Trachyandesite; T-Trachyte and Trachydacite; F-Feldspathoidite; U1-Tephrite and Basanite; U2-Phonolitic Tephrite; U3-Tephritic Phonolite; Ph-Phonolite; Ab-Alkaline basalt; Ar-Alkaline rhyolite; and Sb-Subalkaline basalt).

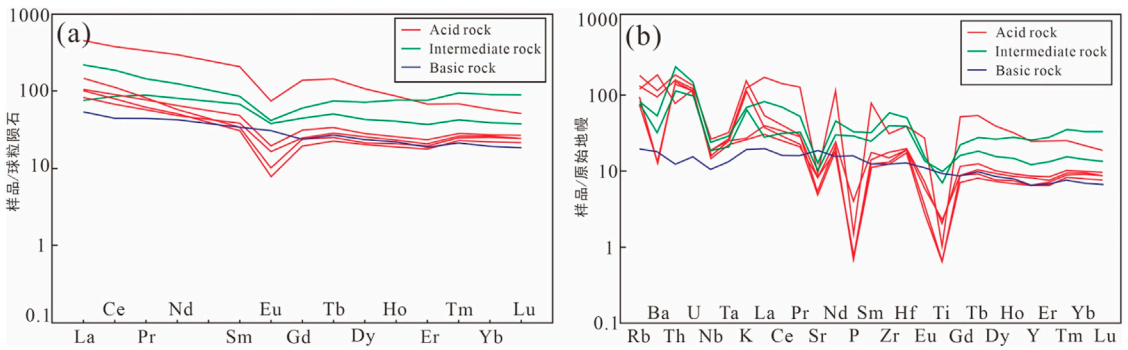

FIGURE 9 | Chondrite-normalized REE patterns **(A)** and primitive mantle-normalized trace element patterns **(B)** for the Carboniferous volcanic rocks in the Shixi area.

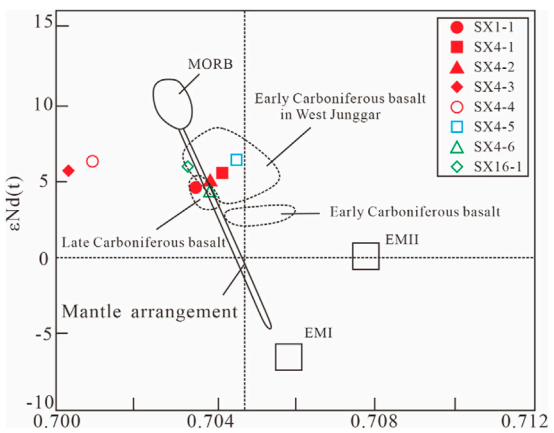

FIGURE 10 | Sr-Nd isotopic characteristics of Carboniferous volcanic rocks in the Shixi area.

lithophile elements and depleted in high-field-strength elements. In addition, the samples have obvious negative Nb and Ta anomalies, positive Pb anomalies, no obvious fractionation of heavy rare earth elements, and high εNd(t) values, which also indicates that the intermediate magma came from the partial melting of the young basic lower crust.

5.1.3 Formation Mechanism of Acid Magma

On the basis of excluding the origin of basic magma fractional crystallization, the low Sr/Y values of acid volcanic rocks indicate that they are not derived from the enriched lithospheric mantle. Low Mg# values (0.19–0.27), low Nb contents (9.98–17.8 ppm), low Nb/La values (0.1648–0.5207), and low $(Ce/Pb)_N$ values (0.088–0.43) indicate that the acid magma is the product of crust melting. The high εNd(t) values (4.87–5.95) indicate that acid magma originated from the young lower crust. Therefore, the acid magma in the Shixi area was formed by partial melting of the young lower crust.

5.2 Volcanic Eruption Pattern

The Carboniferous Junggar basin was formed and developed in the process of subduction and closing of the Paleo-Asian Ocean (Zheng M. L. et al., 2019; Zheng Z. H. et al., 2019; Hou et al., 2020; Xu and Gao, 2020; Wang et al., 2021). In the early Early Carboniferous, the Junggar Basin inherited the Devonian oceanic crust subduction pattern, which was characterized by several ocean basins separated by island arcs. The Kalamiri Ocean was subducted toward the Luliang island arc, and the subduction plate dehydrated and melted to form basic magma. Basic magma rose into the mantle wedge and was retained at the bottom of the crust to form basic magma chambers. In addition, basic magma baked the overlying crust causing partial melting of crustal materials, which then rose to the shallow layer and accumulated into intermediate-acid magma chambers. In the late Early Carboniferous, the retreat of the subduction plate formed an extensional environment in the Luliang island arc, resulting in the development of rifting in the island arc (Tang et al., 2015; He et al., 2018; Yin and Ding, 2019). At this point, volcanic activities began to increase. In the early to middle of the Late Carboniferous, the further retreat of the subduction plate prompted the reactivation of the previous faults, resulting in more intense volcanic activities than in the Early Carboniferous. Intermediate-acid magma upwelled along the Shixi fault and Mobei fault and then formed central eruptions along the secondary faults or melt-through strata, and beaded volcanic edifices along the strike of the faults were developed on the hanging walls of the faults. Affected by fault development, the Shixi fault volcanic belt developed intermediate-acid stratovolcanic edifices and mound superimposed volcanic edifices, while the Mobei fault volcanic belt was dominated by stratovolcanic edifices. The Dinan fault connected with the basic magma chambers. As a banded volcanic vent, the Dinan fault led to fissure eruption, forming widely distributed shield basic volcanic edifices.

6 CONCLUSION

1) The types of Carboniferous volcanic edifices in the Shixi area of the Junggar Basin mainly include stratovolcanic edifices, shield basic volcanic edifices, and mound superimposed volcanic edifices. Stratovolcanic edifices are the most developed in the Shixi area, shield basic volcanic edifices are the least and only distributed in the south of the Shixi area, and the autoclastic breccia belts are developed near the volcanic vents. The volcanic vents extend in tree shapes in space and are well developed in the mound superimposed volcanic edifices. Moreover, cryptoexplosive breccia belts and blowhole lavas are well developed in mound superimposed volcanic edifices.

2) The intermediate-acid magma mainly erupted in a center type along the Shixi and Mobei faults in the study area. The faults control the types and numbers of volcanic edifices. The types of volcanic edifices around the Shixi fault are mainly stratovolcanic edifices and mound superimposed volcanic edifices, while mound superimposed volcanic edifices around the Mobei fault are not developed; only stratovolcanic edifices are developed. The number of volcanic edifices in the Shixi salient is more than that of the Mobei salient. The volcanic edifices are mainly developed on the hanging walls of the faults, which leads to the thicker volcanic strata on the hanging walls. The intermediate-acid volcanic edifices are beaded along one side of the Shixi fault and Mobei fault. The shield basic volcanic edifices are distributed in the northwest direction along both sides of the Dinan fault.

3) The Junggar Basin inherited the oceanic crust subduction pattern of the Devonian, which was characterized by several ocean basins separated by island arcs. The subduction plate dehydrated and melted to form basic magma, and basic magma rose into the mantle wedge and retained at the bottom of the crust to form basic magma chambers. The basic magma baked the overlying crust, causing partial melting of the crustal materials, which then rose to the shallow layer and accumulated into intermediate-acid magma chambers. In the late Early Carboniferous, the extensional environment caused by the retreat of the subduction plate resulted in the development of a large number of faults in the Shixi area. The late tectonic movements reactivated the basement faults, resulting in large-scale volcanic eruptions.

DATA AVAILABILITY STATEMENT

The raw data supporting the conclusions of this article will be made available by the authors, without undue reservation.

AUTHOR CONTRIBUTIONS

AY and AL are responsible for the idea, writing, and revision of this article. BB, LL, and HC are responsible for the data analysis and drawing. XS and JY are responsible for reviewing and editing.

FUNDING

This article is supported by the 14th Five-year Major Project of CNPC “Continental Deep and Ultra-Deep Oil and Gas Enrichment Law and Exploration Evaluation Research” (2021DJ0206).

REFERENCES

Aldanmaz, E., Pearce, J. A., Thirlwall, M. F., and Mitchell, J. G. (2000). Petrogenetic Evolution of Late Cenozoic, Post-collision Volcanism in Western Anatolia, Turkey. *J. Volcanol. Geotherm. Res.* 102, 67–95. doi:10.1016/S0377-0273(00)00182-7

Chen, S. M. (2015). Hydrocarbon Migration and Accumulation Mechanism of Volcanic Reservoirs in Eastern and Western China. *Nat. Gas. Ind.* 35 (4), 16–24. doi:10.3787/j.issn.1000-0976.2015.04.003

Dai, J. J., Luo, J. L., He, X. Y., Ma, S. W., Wang, C., and Xu, X. L. (2020). Oil and Gas Characteristics and Petrogenetic Evolution of the Carboniferous Volcanic Lava in Xiquan Area, Junggar Basin. *Geol. China* 47 (3), 742–754. doi:10.12029/gc20200313

Fan, C., Li, H., Qin, Q., He, S., and Zhong, C. (2020). Geological Conditions and Exploration Potential of Shale Gas Reservoir in Wufeng and Longmaxi Formation of Southeastern Sichuan Basin, China. *J. Pet. Sci. Eng.* 191, 107138. doi:10.1016/j.petrol.2020.107138

Gao, F. (2019). Use of Numerical Modeling for Analyzing Rock Mechanic Problems in Underground Coal Mine Practices. *J. Min. Strata Control Eng.* 1 (1), 013004. doi:10.13532/j.jmsce.cn10-1638/td.2019.02.009

Geng, H., Sun, M., Yuan, C., Zhao, G., and Xiao, W. (2011). Geochemical and Geochronological Study of Early Carboniferous Volcanic Rocks from the West Junggar: Petrogenesis and Tectonic Implications. *J. Asian Earth Sci.* 42, 854–866. doi:10.1016/j.jseaes.2011.01.006

Gong, W. C., Zhang, X. G., Shi, C., Duan, X. X., and Liu, J. S. (2019). Seismic Identification and Analysis of the Volcanic Mechanism of the Huoshiling Formation in the Yingshan Sag, Northern Songliao Basin. *Contemp. Chem. Ind.* 48 (4), 791–794. doi:10.13840/j.cnki.cn21-1457/tq.2019.04.034

He, D. F., Zhang, L., Wu, S. T., Li, D., and Zhen, Y. (2018). Tectonic Evolution Stages and Features of the Junggar Basin. *Oil Gas Geol.* 39 (5), 845–848. doi:10.11743/ogg20180501

He, D., Li, J. H., Liu, S. J., and Han, L. (2009). Research on the Types of Volcanic Structures and Eruption Patterns of the Lower Cretaceous Yingcheng Formation in the Xujiaweizi Fault Depression in the Northern Songliao Basin. *Acta Petrol. Sin.* 25 (3), 659–666. doi:10.1007/s12182-012-0227-4

Hou, E., Cong, T., and Xie, X. (2020). Ground Surface Fracture Development Characteristics of Shallow Double Coal Seam Staggered Mining Based on Particle Flow. *J. Min. Strata Control Eng.* 2 (1), 013521. doi:10.13532/j.jmsce.cn10-1638/td.2020.01.002

Hu, J., Wang, L. W., Zhang, S. J., Pi, X., Chi, H. Z., Xing, C., et al. (2018). Establishment Method and Application of Geological Model of Volcanic Institutions in the Basin: Taking Yingcheng Formation Volcanic Rocks in Southern Songliao Basin as an Example. *J. Xi'an Shiyou Univ. (Natural Science Edition)* 33 (6), 18–26. doi:10.3969/j.issn.1673-064X.2018.06.003

Huang, W. L., Wang, P. J., Feng, Z. Q., Shao, R., Guo, Z. H., and Xu, Z. J. (2007). Analogy of Volcanic Edifices between Modern Volcanoes and Ancient Remnant Volcanoes in Songliao Basin. *J. Jilin Univ. (Earth Science Edition)* 37 (1), 65–72. doi:10.13278/j.cnki.jjuese.2007.01.011

Huang, Y., Liang, S. Y., Jia, C. M., Gu, X. P., Mao, H. B., and Fu, X. P. (2020). Identification of Palaeovolcanic Structures and Practice of Oil and Gas Exploration in the Reconstruction of the Junggar Basin. *Nat. Gas. Ind.* 40 (3), 30–37. doi:10.3787/j.issn.1000-0976.2020.03.004

Lan, S. R., Song, D. Z., Li, Z. L., and Liu, Y. (2021). Experimental Study on Acoustic Emission Characteristics of Fault Slip Process Based on Damage Factor. *J. Min. Strata Control Eng.* 3 (3), 033024. doi:10.13532/j.jmsce.cn10-1638/td.20210510.002

Li, H., Li, J., Xu, X. Y., Yang, G. X., Wang, Z. P., Xu, Q., et al. (2021). Petrogenesis and Tectonic Implications of Alkali Basalts in Kalamaili Area, East Junggar, Xinjiang (NW China): Constraints from Petrology, Geochronology and Geochemistry. *Acta Geol. Sin.* 95 (11), 3282–3300. doi:10.19762/j.cnki.dizhixuebao.2020281

Li, H., Qin, Q., Zhang, B., Ge, X., Hu, X., Fan, C., et al. (2020a). Tectonic Fracture Formation and Distribution in Ultradeep Marine Carbonate Gas Reservoirs: A Case Study of the Maokou Formation in the Jiulongshan Gas Field, Sichuan Basin, Southwest China. *Energy Fuels* 34 (11), 14132–14146. doi:10.1021/acs.energyfuels.0c03327

Li, H. (2022). Research Progress on Evaluation Methods and Factors Influencing Shale Brittleness: A Review. *Energy Rep.* 8, 4344–4358. doi:10.1016/j.egyr.2022.03.120

Li, H., Tang, H., Qin, Q., Zhou, J., Qin, Z., Fan, C., et al. (2019). Characteristics, Formation Periods and Genetic Mechanisms of Tectonic Fractures in the Tight Gas Sandstones Reservoir: A Case Study of Xujiahe Formation in YB Area, Sichuan Basin, China. *J. Pet. Sci. Eng.* 178, 723–735. doi:10.1016/j.petrol.2019.04.007

Li, L., Zhang, X., and Deng, H. (2020b). Mechanical Properties and Energy Evolution of Sandstone Subjected to Uniaxial Compression with Different Loading Rates. *J. Min. Strata Control Eng.* 2 (4), 043037. doi:10.13532/j.jmsce.cn10-1638/td.20200407.001

Li, S. B., Guo, X. G., Zheng, M. L., Wang, Z. S., and Liu, X. L. (2021). Lithology Identification of Carboniferous Volcanic Rocks in Xiquan Area, Eastern Junggar Basin. *Lithol. Reserv.* 33 (1), 258–266. doi:10.12108/yxyqc.20210124

Li, Z. (2019). *Study on Reservoir Characteristics of Carboniferous Volcanic Weathering Crust in Shixi Oilfield, Central Junggar Basin*. Chengdu: Southwest Petroleum University, 22–36. doi:10.27420/d.cnki.gxsyc.2019.000185

Lu, J. L., Zuo, Z. X., Shi, Z., Dong, X., Wu, Q., and Wu, Q. J. (2019). Characteristics of Permian Volcanism and Natural Gas Exploration Potential in Western Sichuan Basin. *Nat. Gas. Ind.* 39 (2), 46–53. doi:10.3787/j.issn.1000-0976.2019.02.006

Luo, B., Xia, M. L., Wang, H., Fan, Y., Xu, L., Liu, R., et al. (2013). Hydrocarbon Accumulation Conditions of Permian Volcanic Gas Reservoirs in the Western Sichuan Basin. *Nat. Gas. Ind.* 39 (2), 9–16. doi:10.3787/j,issn.1000-0976.2019.02.002

Ma, L. M., Li, Z. P., Lin, C. Y., Dong, B., Bu, L. X., and Cui, L. (2013). Jurassic Structural Style and its Oil Control Rule in Dzungar Basin Field. *Petroleum Geol. Xinjiang* 34 (1), 27–29. doi:10.1080/10916466.2019.1702688

Ma, X. H., Yang, Y., Zhang, J., and Xie, J. R. (2019). A Major Discovery in Permian Volcanic Rock Gas Reservoir Explorationin the Sichuan Basin and its Implications. *Nat. Gas. Ind.* 39 (2), 1–8. doi:10.1016/j.ngib.2019.02.001

Meng, F. C., Zhou, L. H., Wei, J. Y., Cui, Y., Lou, D., Chen, S. Y., et al. (2021). Characteristics and Formation Mechanism of Mesozoic Volcanic Reservoirsfrom Buried Hills in Huanghua Depression, Bohai Bay Basin. *J. Central South Univ. Sci. Technol.* 52 (3), 859–875. doi:10.11817/j.issn.1672-7207.2021.03.019

Qu, Y. (2019). Structural Fractures and Geostress in Volcanic Rocks of Yingcheng Formation, D Block, Xushen Gasfield, Songliao Basin. *Nat. Gas Explor. Dev.* 42 (1), 28–34. doi:10.12055/gaskk.issn.1673-3177.2019.01.005

Safonova, I., Kojima, S., Nakae, S., Romer, R. L., Seltmann, R., Sano, H., et al. (2015). Oceanic Island Basalts in Accretionary Complexes of SW Japan: Tectonic and Petrogenetic Implications. *J. Asian Earth Sci.* 113, 508–523. doi:10.1016/j.jseaes.2014.09.015

Shan, X. L., Chen, Y. P., Tang, L. M., and Yi, J. (2011). Comprehensive Evaluation Method for Volcanic Rock Reservoirs and its Application: Taking Songnan Gas Field for Example. *J. Shandong Univ. Sci. Technol.* 30 (3), 1–6. doi:10.16452/j.cnki.sdkjzk.2011.03.001

Tamura, Y., Ishizuka, O., Stern, R. J., Nichols, A. R. L., Kawabata, H., Hirahara, Y., et al. (2014). Mission Immiscible: Distinct Subduction Components Generate Two Primary Magmas at Pagan Volcano, Mariana Arc. *J. Petrology* 55 (1), 63–101. doi:10.1093/petrology/egt061

Tang, H. F., Wang, P. J., Bian, W. H., Huang, Y. L., Gao, Y. F., and Dai, X. J. (2020). Review of Geological Research on Volcanic Rock Reservoirs. *Chin. J. Petroleum* 32 (5), 1744–1773. doi:10.7623/syxb202012026

Tang, H. F., Wang, P. J., Li, R. L., Huang, C., and Bai, B. (2012). Classification of Volcanic Edifices and its Characteristics of Gas Pool in Faulted Sequence of the Songliao Basin, NE China. *J. Jilin Univ. (Earth Science Edition)* 42 (3), 583–589. doi:10.13278/j.cnki.jjuese.2012.03.001

Tang, Y., Wang, G., Zheng, M, L., Chen, L., Feng, L., Kong, Y. H., et al. (2015). Carboniferous Basin Evolution and its Hydrocarbon Accumulation in the North of Xinjiang. *Earth Sci. Front.* 22 (3), 241–253. doi:10.13745/j.esf.2015.03.021

Wang, L., Xu, Y. D., Zhang, Y. J., Liu, Z. C., and Shang, F. K. (2020). Main Controlling Factors and Development Model of Carboniferous Reservoirs in Chepaizi Uplift, Junggar Basin. *J. Northeast Petroleum Univ.* 44 (2), 79–90. doi:10.3969/j.issn.2095-4107.2020.02.008

Wang, X. J., Song, Y., Zheng, M. L., Ren, H. J., Wu, H. S., He, W. J., et al. (2021). Composite Petroleum System and Multi-Stage Hydrocarbon Accumulation in Junggar Basin. *China Pet. Explor.* 26 (4), 29–43. doi:10.3969/j.issn.1672-7703.2021.04.003

Wang, X. Y., Liu, Q. H., Zhu, H. T., Hou, G. W., and Qin, L. Z. (2020). Three-dimensional Sculpture and Genetic Mechanism Analysis of Volcanic Structures in the Tiantai Slope Zone of Xihu Sag. *Bull. Geol. Sci. Technol.* 40 (4), 72–80. doi:10.19509/j.cnki.dzkq.2021.0406

Xia, M. L., Wen, L., Li, Y., Luo, B., He, K. L., Liu, R., et al. (2020). Permian Volcanic Eruption Cycle, Environment and Model in the Jianyang Area of the Sichuan Basin. *Nat. Gas. Ind.* 40 (9), 11–22. doi:10.3787/j.issn.1000-0976.2020.09.002

Xu, N., and Gao, C. (2020). Study on the Special Rules of Surface Subsidence Affected by Normal Faults. *J. Min. Strata Control Eng.* 2 (1), 011007. doi:10.13532/j.jmsce.cn10-1638/td.2020.01.011

Yi, J., Shan, X. L., Tang, H. F., Zhang, Y. Y., and Chen, Y. P. (2011). The Geological-Geophysical Two-Dimensional Dissection of Basin Buried Volcanic Edifices-Take the First Member of Yingcheng Formation in Yaoyingtai Region of Southern Songliao Basin as an Example. *Chin. J. Geophys.* 54 (2), 587–596. doi:10.3969/j.issn.0001-5733.2011.02.038

Yin, S., and Ding, W. L. (2019). Evaluation Indexes of Coalbed Methane Accumulation in the Strong Deformed Strike-Slip Fault Zone Considering Tectonics and Fractures: A 3D Geomechanical Simulation Study. *Geol. Mag.* 156 (6), 1–17. doi:10.1017/s0016756818000456

Yin, S., Xie, R., Wu, Z., Liu, J., and Ding, W. (2019). *In Situ* stress Heterogeneity in a Highly Developed Strike-Slip Fault Zone and its Effect on the Distribution of Tight Gases: A 3D Finite Element Simulation Study. *Mar. Petroleum Geol.* 99 (1), 75–91. doi:10.1016/j.marpetgeo.2018.10.007

You, X. C., Gao, G., Wu, J., Zhao, J. Y., Liu, S. J., and Duan, Y. J. (2021). Differences of Effectivity and Geochemical Characteristics of the Fengcheng Formation Source Rock in Ma'nan Area of the Junggar Basin. *Nat. Gas. Geosci.* 32 (11), 1697–1708. doi:10.11764/j.issn.1672-1926.2021.08.002

Zhang, S. Y., Zhu, J., Wen, G., Liu, S. Q., Lu, X. C., Zhang, S. C., et al. (2015). Significant of Volcanic Eruption Spatiotemporal Sequence in Batamayineishan Formation, Ludong Region, Junggar Basin. *J. Central South Univ. Sci. Technol.* 46 (1), 199–207. doi:10.11817/j.issn.1672−7207.2015.01.027

Zhao, N., and Shi, Q. (2012). Characteristics of Fractured and Porous Volcanic Reservoirs and the Major Controlling Factors of Their Physical Properties: A Case Study from the Carboniferous Volcanic Rocks in Ludong-Wucaiwan Area, Junggar Basin. *Nat. Gas. Ind.* 32 (10), 14–23. doi:10.3787/j.issn.1000-0976.2012.10.004

Zheng, M. L., Fan, X. D., He, W. J., Yang, T. Y., Tang, Y., Ding, J., et al. (2019a). Superposition and Evolution of Deep Geological Structure and Hydrocarbon Accumulation in Junggar Basin. *Earth Sci. Front.* 26 (1), 22–32. doi:10.13745/j.esf.sf.2019.1.2

Zheng, Z. H., Du, S. K., Liao, J. B., Chen, H. Y., and Yu, H. G. (2019b). Drops of West Region in Junggar Basin Carboniferous Igneous Rock Gas Reservoir Capacity Main Control Factors. *J. China Univ. Min.* 13 (3), 604–615. doi:10.13247/j.cnki.jcumt.000955

Zhu, W., Niu, L., and Li, S. (2019). Creep-impact Test of Rock: Status-Of-The-Art and Prospect. *J. Min. Strata Control Eng.* 1 (1), 013003. doi:10.13532/j.jmsce.cn10-1638/td.2019.02.007

Zou, C.-N., Zhao, W.-Z., Jia, C.-Z., Zhu, R.-K., Zhang, G.-Y., Zhao, X., et al. (2008). Formation and Distribution of Volcanic Hydrocarbon Reservoirs in Sedimentary Basins of China. *Petroleum Explor. Dev.* 35 (3), 257–271. doi:10.1016/s1876-3804(08)60071-3

Conflict of Interest: The authors AY, BB, LL, and HC were employed by the PetroChina Xinjiang Oilfield Company.

The remaining authors declare that the research was conducted in the absence of any commercial or financial relationships that could be construed as a potential conflict of interest.